

Field-Simulation Based Engineering of RF Antenna Probes with Non-Uniform Substrates for High-Field Magnetic Resonance Imaging Systems

Navid P. Gandji, Akshay V. Palle, George B. Semouchkin, and Elena Semouchkina

Department of Electrical and Computer Engineering
Michigan Technological University, Houghton, Michigan 49931, USA
npourram@mtu.edu, apalle@mtu.edu, gbsemouc@mtu.edu, esemouch@mtu.edu

Abstract — It is proposed to replace RF volume coils in high-field Magnetic Resonance Imaging (MRI) scanners by a microstrip patch antenna system. The performed computational studies have demonstrated an opportunity to form extended 3D volumes of homogenous RF magnetic fields by using a system of placed *vis-à-vis* two patch antennas. In order to control antenna dimensions and homogeneity of antenna near fields, the substrates of antennas have been engineered by appropriate patterning of high permittivity dielectric inserts. A variety of antennas with engineered substrates responding at 600 MHz for application in 14T MRI scanners have been designed, and the homogeneity of magnetic fields achieved inside the antenna system has been demonstrated.

Index Terms — High-field MRI systems, magnetic field uniformity, patch antenna, RF probe.

I. INTRODUCTION

Magnetic resonance imaging (MRI) is a major tool for investigating a comprehensive range of biological systems from single cells to humans. The advantage of high-field MRI scanners is their potential to provide higher signal-to-noise ratio and, consequently, improved anatomic and temporal resolution [1]. Major advancements are anticipated, in particular, for animal and plant imaging carried out in MRI scanners with the strength of the applied static magnetic field B_0 exceeding 7T. Employing higher magnetic fields leads to increased Larmor frequency, which characterizes the precession of nuclear magnetic moments around the direction of B_0 . In particular, in 14T systems this frequency is equal to 600 MHz. RF coils, serving for both transmitting and receiving functions in MRI, generate an oscillating magnetic field B_1 , which is normal to B_0 . If oscillations of the B_1 field match the Larmor frequency, the energy of the B_1 field can be effectively transmitted to the nuclear spin system. The performance of conventional volume coils, such as birdcage coils [2], degrades at high frequencies in the high field MRI, since dimensions of

coils become large compared to wavelengths, so that wave phenomena take place. As a result, obtaining a spatially homogeneous magnetic field covering a larger field of view (FOV) that is required for high image quality becomes a principal challenge [3].

Recently, it was proposed to apply a microstrip patch antenna for excitation of circularly polarized travelling wave in the scanner's bore that acted as a waveguide, with expectations to provide a more homogeneous fields over larger FOV compared to that achieved by using conventional volume coils. However, this approach demonstrated relatively poor transmit efficiency and receive sensitivity, therefore, it was proposed to add multi-channel receive-only arrays to increase the sensitivity [4, 5]. In order to decrease patch antenna size for fitting it inside a 16.4T magnet bore, a substrate of high relative permittivity ($\epsilon_r = 9.6$) was used that decreased radiation efficiency. In addition, high cutoff frequency for the dominant mode of the magnet bore in 16.4T scanner did not allow for supporting wave propagation at 698 MHz, so only an evanescent wave was generated [4].

In this work we propose to substitute volume coils in 14T MRI scanner operating at 600 MHz by a system of two microstrip patch antennas. The system is, in particular, applicable for small animal imaging. The target of the design is to produce extended 3D volumes of highly homogeneous and strong magnetic fields inside the system of miniaturized antennas with engineered multi-dielectric substrates. The transient solver of the commercial software package CST Microwave studio was used for conducting full-wave electromagnetic simulations to control antenna near fields, characterize antenna performance, and guide antenna substrate engineering. The field post-processing option of the CST solver was employed to plot the curves of spatial field distribution.

II. DESIGNING PATCH ANTENNA SYSTEM

Figure 1 presents the schematic of the projected placement of two patch antennas in 14T magnet bore

with the diameter of 5.4 cm. The dimensions of the antenna system were chosen to accommodate an object between two patches with the size of about 2 cm × 2 cm (representing the head of a mouse), so that the antenna substrate had a square shape and the area of 3 cm × 3 cm while the separation between two patches was 2 cm. The patch electrodes had rectangular shape with the length L along Z axis and the width W along X -axis, so that B_1 field produced by the antenna at the half-wavelength resonance along the patch length was directed along X -axis, i.e., normal to B_0 oriented along Z -axis (Fig. 1).

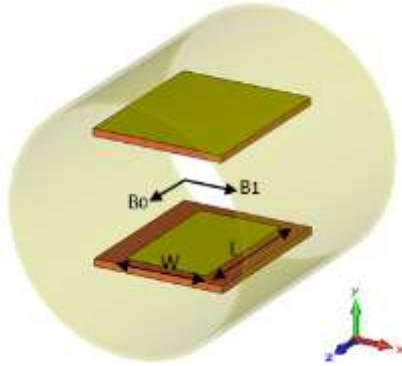


Fig. 1. Schematic of patch antenna placement in the magnet bore.

A. Conventional patch antenna with uniform substrate

It is known that the length of rectangular patch electrode of a microstrip patch antenna is related to its operation frequency f at the half-wavelength resonance by the expression:

$$L = \frac{\lambda}{2} = \frac{c_0}{2f \sqrt{\epsilon_r^{eff}}}, \quad (1)$$

where c_0 is the speed of light in free space and ϵ_r^{eff} is the effective permittivity of the substrate defined by the relative permittivity of the substrate (ϵ_r), height (H) of the substrate and width (W) of the patch electrode [6].

As the first step in developing patch antenna for 14T MRI system operating at 600 MHz, an antenna with uniform substrate made of a typical material Arlon ($\epsilon_r = 3$, $\tan \delta \approx 0.028$) [7] was designed. Figure 2 (a) presents the schematic of the antenna fed by a 50-ohms coaxial probe, where the feed point location was optimized to provide impedance matching. The S_{11} and the fringing field spectra shown in Fig. 2 (b) demonstrate that the antenna does radiate at 600 MHz. The dimensions of this antenna, however, were $L' \times W' = 17 \text{ cm} \times 13 \text{ cm}$ at the substrate height (H) of 1.6 mm, while the patch electrode dimensions were $L \times W = 13 \text{ cm} \times 10 \text{ cm}$. It is obvious that such conventional patch antenna cannot fit in the magnet bore with the diameter of 5.4 cm. Although, according to (1), the antenna size could be decreased by using a substrate of high permittivity material, this would

lead to pulling fields inside the substrate at the expense of fields outside antenna.

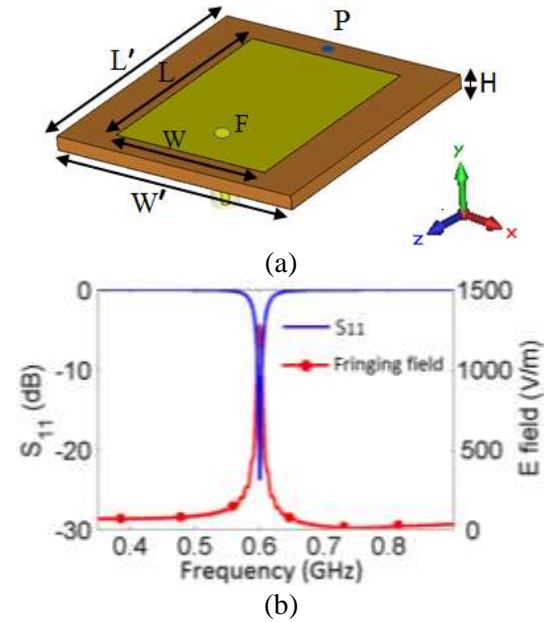


Fig. 2. (a) Antenna schematic and (b) S_{11} of the antenna and the spectrum of the fringing E-field magnitude sampled at point P located at 1.5 mm distance from the patch edge. The point F denotes the optimised feed location.

In our earlier work [8, 9] we proposed to use a substrate composed of a combination of low and high permittivity materials for both shrinking the antenna size and manipulating its characteristics. In the following sections we show how, based on the analysis of simulated field distributions, non-uniform substrates could be designed to provide uniform and strong magnetic near fields and desired antenna size for its application in the MRI system.

B. Patch antenna with one high permittivity insert inside the low permittivity substrate

For the first design of a miniaturized antenna we followed our approach proposed in [8] to insert a rectangular plug of a material with high permittivity such as Calcium Titanate ($\epsilon_r = 170$, $\tan \delta \approx 0.004$) into Arlon substrate with the thickness of 1.6 mm, so that dimensions of the plug were smaller than the patch dimensions in order to minimize fringing field distortion. Targeting the operation frequency of 600 MHz and the area of the substrate of $L' \times W' = 3 \text{ cm} \times 3 \text{ cm}$, the chosen combination of materials allowed for designing the antenna with the patch electrode dimensions $L \times W = 2.4 \text{ cm} \times 1.9 \text{ cm}$, while the dimensions of high permittivity plug after optimization were 2.1 cm × 1.6 cm. The dimension of inserts were chosen to make the effective permittivity

under the patch being close to 110 so that the antenna would resonate at 600 MHz.

The simulated electric field pattern inside the substrate and magnetic field pattern sampled at 10 mm above the patch of the miniaturized antenna are presented in Fig. 3 at the frequency of 600 MHz and at optimized feed location providing matched input impedance of the antenna at this frequency.

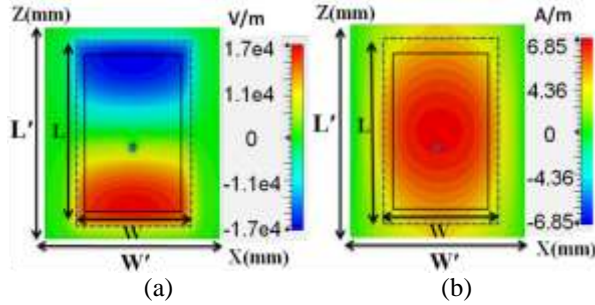


Fig. 3. Distributions of: (a) E_y field component in XZ plane inside the substrate at its half height, and (b) H_x field component in XZ plane located 10 mm above the patch at 600 MHz for the antenna with one high permittivity insert in the substrate. Dashed lines mark the patch electrode and solid lines mark the insert.

The designed antenna has appropriate dimensions to fit in the magnet bore and its magnetic near field, as seen from Fig. 3, covers the major portion of the area above the patch, except for the regions along the boundaries. In the next section we investigate opportunities to further increase the uniformity of near magnetic fields by using multiple high permittivity inserts instead of one in the antenna substrate.

C. Patch antennas with multiple high permittivity inserts in low permittivity substrates

As illustrated by Fig. 3 (a), electric field inside the antenna substrate at the half-wavelength resonance is concentrated in the substrate under the patch edges. Since high permittivity material provides for wave compression by directly influencing electric field, high permittivity inserts located under patch edges should be more efficient for antenna miniaturization, than similar inserts placed under the central part of the patch. Consequently, in order to increase miniaturization efficiency of a non-uniform substrate and to make its fabrication easier, the next step in advancing the antenna design was to use instead of one big high permittivity insert two smaller inserts near substrate edges, where electric field was concentrated (Fig. 4 (a)).

In order to maintain the level of miniaturization with smaller inserts, a higher permittivity insert material was required, which was chosen to be Strontium Titanate ($\epsilon_r = 300$, $\tan \delta \approx 0.002$).

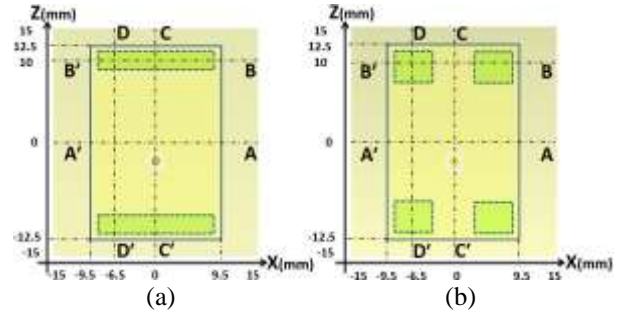


Fig. 4. Schematics of high permittivity insert placement under the patch in antenna substrates: (a) two inserts and (b) four inserts.

Figure 4 (a) shows the schematic of the substrate with two high permittivity inserts having the dimensions of 2 mm \times 18 mm and the thickness of 1.6 mm (equal to the substrate thickness). The inserts with the above parameters were found to provide antenna operation at 600 MHz with the same dimensions of the patch electrode (2.4 cm \times 1.9 cm) as those of the antenna with one big insert. Figure 5 compares magnetic field distributions for antennas with one and two inserts sampled at 10 mm above the patch at 600 MHz and at feed locations in antennas providing for matched input impedance.

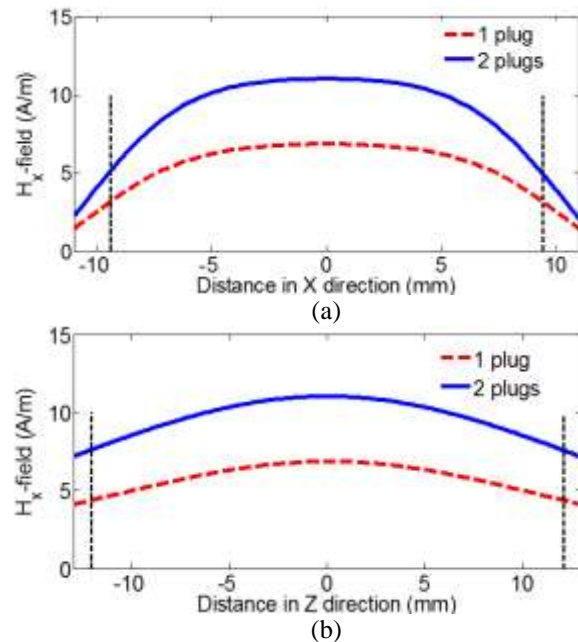


Fig. 5. Distributions of H_x field in XZ plane located 10 mm above patch antennas with one and two inserts: (a) along antenna width (X-direction), i.e., along A-A' in Fig. 4 (a), and (b) along antenna length (Z-direction), i.e., along C-C' in Fig. 4 (a). Vertical dashed lines mark the edges of the patch.

As seen in the Fig. 5, smaller high permittivity inserts, which are easier to fabricate, provide, in addition to similar antenna miniaturization, similar magnetic field uniformity, as one big insert does, and even about twice higher magnitude of magnetic field above the patch. The latter could be related to additional secondary field originating from displacement currents in high permittivity material [10]. Based on the results presented in Fig. 5, it is reasonable to suggest that placing various permittivity materials under patch locally would increase or decrease local magnetic field in a controlled manner. This consideration guided the placement of four high permittivity inserts in the next design of the antenna depicted in Fig. 4 (b).

In order to keep the same dimensions of the antenna for operation at the same frequency of 600 MHz, the dimensions of each of four inserts made of the same material ($\epsilon_r = 300$) as that of the design with two inserts, were found to be: 4 mm \times 4 mm \times 1.6 mm. Figure 6 compares magnetic field distributions for antennas with two and four high permittivity inserts sampled at 10 mm above the patch electrodes at 600 MHz and at feed locations in antennas providing for matched input impedance. Although field distributions were not significantly different, the uniformity of magnetic field along antenna shorter edge was improved, as expected, for antenna with four high permittivity inserts (Fig. 6 (b)).

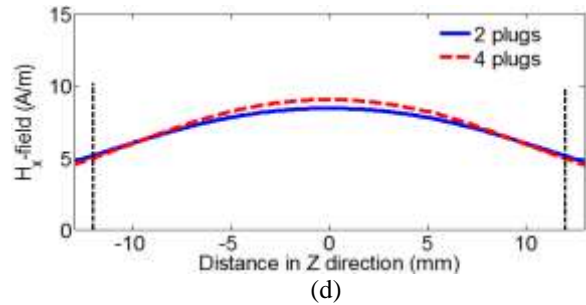
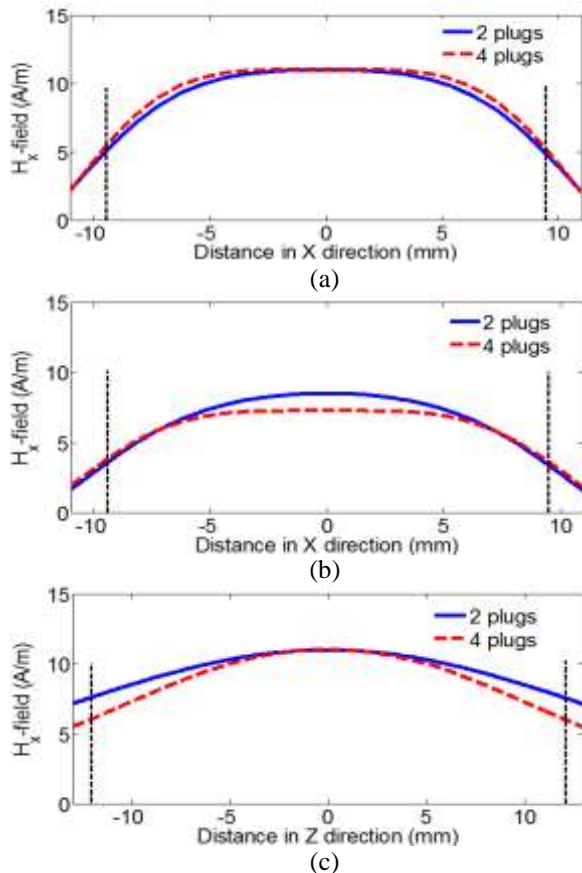


Fig. 6. Distribution of H_x field in XZ plane located 10 mm above patch antennas with two and four inserts along antenna width (X-direction), i.e., along (a) A-A' in Fig. 4 and (b) B-B' in Fig. 4, and along antenna length (Z-direction), i.e., along (c) C-C' in Fig. 4 and (d) D-D' in Fig. 4.

D. Combining miniaturized antennas in an antenna system

As illustrated in Fig. 1, two identical miniaturized patch antennas should be placed *vis-à-vis* in the magnet bore 20 mm apart. Antennas should be excited with 180° phase difference, therefore, their magnetic near fields H_x will add in the space between antennas. Figure 7 (a) presents the distributions of magnetic fields of each antenna and of the field resulting from summation, along the axis normal to the patches within the separation distance between antennas.

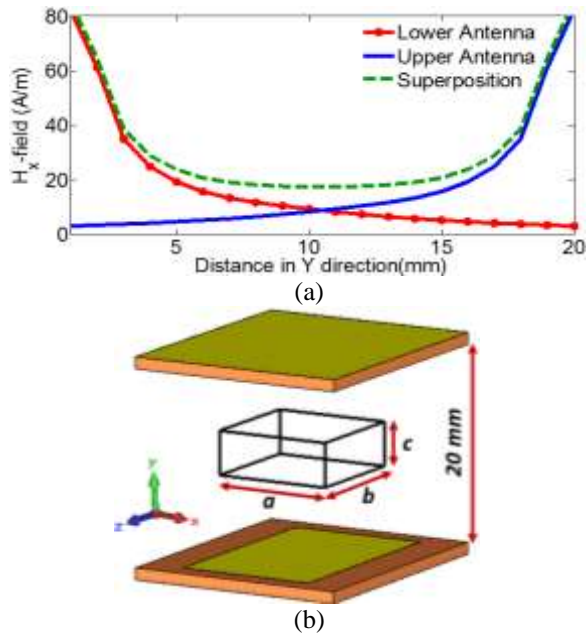


Fig. 7. (a) Distribution of H_x field for each antenna and for the antenna system along the axis normal to patches (Y-axis) within the separation distance of 20 mm between antennas, and (b) schematic of placement of the MRI object with dimensions ($a \times b \times c$) between two antennas.

As seen in Fig. 7 (a), the distribution of the magnetic field in the antenna system along the axis normal to patches demonstrates high uniformity. To illustrate the level of field uniformity in all three directions, Fig. 7 (b) shows the schematic of placement of an MRI object with dimensions ($a \times b \times c$) in the space between two antennas. The uniformity of field can be defined by the ratio of minimal and maximal field strengths along the dimensions of the phantom [11, 12]. Then it can be calculated that the field uniformity in Y-direction, i.e., along the object height c in Fig. 7 (b), when $c = 6$ mm, is almost 97%, while for the object with the height $c = 10$ mm it is 90%. From the results presented in the previous section, it could be obtained that in Z-direction along the object length of 10 mm ($a = 10$ mm) the achieved uniformity is 91%, while in X-direction along the object width of 10 mm ($b = 10$ mm) the uniformity is around 90%. Overall, for a sample with dimensions ($a \times b \times c$) = (10 mm \times 10 mm \times 10 mm) placed between two antennas, the magnetic field uniformity in the volume covered by the object is not less than 90% and is even higher for smaller objects, respectively.

III. CONCLUSION

A system of two microstrip patch antennas has been designed to substitute RF volume coils in 14T MRI system operating at 600 MHz. In order to miniaturize antennas for fitting in the magnet bore with the diameter of 5.4 cm it is proposed to use a combination of two dielectric materials with low and high permittivity in the antenna substrates. Based on the analysis of simulated near fields produced by antenna, several designs of miniaturized antennas have been developed. It is demonstrated that uniformity of the magnetic field within the volume of an object with the dimensions (10 mm \times 10 mm \times 10 mm) placed between two antennas exceeds 90%.

ACKNOWLEDGMENT

This work was supported by the National Science Foundation under Award IDBR-1353664.

The authors also wish to thank Dr. Michael Lanagan and Dr. Thomas Neuberger (The Pennsylvania State University) for helpful discussions.

REFERENCES

- [1] Y. Hyongsuk, G. Anand, and J. T. Vaughan, "A method to control non-uniformity RF B_1 field for high field magnetic resonance imaging," *IEEE MTT-S Int. Microwave Symp. Dig.*, Anaheim, CA, pp. 752-755, May 2010.
- [2] J. T. Vaughan, G. Adriany, C. J. Snyder, J. Tian, T. Thiel, L. Bolinger, H. Liu, L. DelaBarre, and K. Ugurbil, "Efficient high-frequency body coil for high-field MRI," *Magnetic Resonance in Medicine*, 52, pp. 851-859, Sep. 2004.
- [3] J. Hoffmann, J. Budde, G. Shajan, and R. Pohmann, "Slice-selective B_1 phase shimming at 9.4 T," *Proc. Int. Soc. Mag. Reson. Med.*, 18, Stockholm, Sweden, pp. 1470, 2010.
- [4] G. Shajan, J. Hoffmann, D. Z. Balla, D. K. Deelchand, K. Scheffler, and R. Pohmann, "Rat brain MRI at 16.4T using a capacitively tunable patch antenna in combination with a receive array," *NMR in Biomedicine*, vol. 25, no. 10, pp. 1170-1176, 2012.
- [5] J. Hoffmann, G. Shajan, J. Budde, K. Scheffler, and R. Pohmann, "Human brain imaging at 9.4 T using a tunable patch antenna for transmission," *Magnetic Resonance in Medicine*, 69, pp. 1494-1500, 2013.
- [6] H. A. Wheeler, "Transmission-line properties of a strip on a dielectric sheet on a plane," *IEEE Tran. Microwave Theory Tech.*, vol. MTT-25, pp. 631-647, Aug. 1977.
- [7] T. Reynalda, A. Munir, and E. Bharata, "Characterization of 4x4 high gain microstrip array antenna for 3.3GHz WiMAX application," *IEEE TSSA, 6th Int. Conference*, Bali, Indonesia, pp. 215-218, Oct. 2011.
- [8] E. Semouchkina, A. Baker, G. Semouchkin, T. Kerr, and M. Lanagan, "Wearable patch antenna for voice communications with substrate composed of high contrast dielectrics," *IEEE APS Int. Symp.*, Honolulu, HI, pp. 4188-4191, June 2007.
- [9] E. Semouchkina, J. Scholz, S. Perini, G. B. Semouchkin, M. Lanagan, R. Haupt, and H. Simonds, "Metamaterials inspired miniaturization of UHF patch antennas with circular polarization," *Microwave and Optical Technology Letters*, vol. 53, no. 8, pp. 1938-1943, Aug. 2011.
- [10] W. M. Brink, R. F. Remis, and A. G. Webb, "A theoretical approach based on electromagnetic scattering for analyzing dielectric shimming in high-field MRI," *Magnetic Resonance in Medicine*, June 2015.
- [11] X. Chen, "Analytical path to improved RF field homogeneity for high field MRI," *Ph.D. Thesis*, Department of Physics, CASE Western Reserve University, 2009.
- [12] J. T. Vaughan, M. Garwood, C. M. Collins, W. Liu, L. DelaBarre, G. Adriany, P. Andersen, H. Merkle, R. Goebel, M. B. Smith, and K. Ugurbil, "7T vs. 4T: RF power, homogeneity, and signal-to-noise comparison in head images," *Magnetic Resonance in Medicine*, vol. 46, no. 1, pp. 24-30, Jan. 2001.



Navid P. Gandji received the M.S. degree in Microwave Communication Engineering from Iran University of Science and Technology, Tehran, Iran, in 2009.

He is currently a Ph.D. degree candidate in Electrical Engineering with Michigan Technological University. His research interests include designing antennas and filters, and metamaterials.



Akshay V. Palle received the Bachelor of Technology degree in Electronics and Communication Engineering from Jawaharlal Nehru Technological University, Hyderabad, India, in 2014.

He is currently a M.S. degree candidate in Electrical Engineering with Michigan Technological University. His research interests include designing antennas and microwave structures.



George Semouchkin received the M.S. degree in Electrical Engineering, Ph.D. degree in Materials, and Doctor of Science degree in Physics and Mathematics from Leningrad Polytechnic Institute (now St. Petersburg State Technical University), St. Petersburg, Russia, in 1962, 1970, and 1990, respectively.

He is currently Research Professor of Electrical Engineering with Michigan Technological University. Prior to joining Michigan Technological University in 2010, he was a Visiting Professor of Materials with the Materials Research Institute, the Pennsylvania State University, University Park, from 1999, and, earlier he was with the St. Petersburg State Technical University, Russia, as a Professor, a Leading Scientist, a Head of the Laboratory, and a Senior Scientist, where he studied ionic crystals, ceramic materials, inorganic dielectrics and developed microelectronic devices. He has authored over 150 technical publications. His current research interests include microwave devices and all-dielectric metamaterials.



Elena Semouchkina received the M.S. degree in Electrical Engineering and the Ph.D. degree in Physics and Mathematics from Tomsk State University, Tomsk, Russia, in 1978 and 1986, respectively, and the Ph.D. degree in Materials from The Pennsylvania State University,

University Park, in 2001.

She is currently Associate Professor of Electrical Engineering and Adjunct Professor of Physics with Michigan Technological University, as well as Adjunct Professor with the Pennsylvania State University. Prior to working at the Materials Research Institute, the Pennsylvania State University, from 1997 to 2009, initially as a Graduate Research Assistant, then as a Postdoctoral Scholar, later as a Research Associate, and, then as a Senior Research Associate and Associate Professor, she was a Scientist with Russian academic centers, such as the Siberian Physics-Technical Institute, St. Petersburg State Technical University, and Ioffe Physics-Technical Institute, where she was involved with the investigation of metal-oxide-semiconductor devices and the development of infrared photodetectors. She has authored and co-authored over 80 publications in scientific journals. Her current research interests are focused on electromagnetic analysis of microwave materials, metamaterials and devices.

Semouchkina was a recipient of the best Ph.D. Thesis Award of the Materials Research Institute at The Pennsylvania State University in 2001 and the National Science Foundation 2004 Advance Fellows Award.